



LAWRENCE
LIVERMORE
NATIONAL
LABORATORY

Investigations of the impact of cross-field drifts on divertor detachment in DIII-D with UEDGE

A. E. Jarvinen, S. L. Allen, M. Groth, A. G. McLean, T. D. Rognlien, C. M. Samuel, A. Briesemeister, M. Fenstermacher, D. N. Hill, A. W. Leonard, G. D. Porter

June 22, 2016

43rd European Physical Society Conference on Plasma Physics
Leuven, Belgium
April 4, 2016 through April 8, 2016

Disclaimer

This document was prepared as an account of work sponsored by an agency of the United States government. Neither the United States government nor Lawrence Livermore National Security, LLC, nor any of their employees makes any warranty, expressed or implied, or assumes any legal liability or responsibility for the accuracy, completeness, or usefulness of any information, apparatus, product, or process disclosed, or represents that its use would not infringe privately owned rights. Reference herein to any specific commercial product, process, or service by trade name, trademark, manufacturer, or otherwise does not necessarily constitute or imply its endorsement, recommendation, or favoring by the United States government or Lawrence Livermore National Security, LLC. The views and opinions of authors expressed herein do not necessarily state or reflect those of the United States government or Lawrence Livermore National Security, LLC, and shall not be used for advertising or product endorsement purposes.

Investigations of the impact of cross-field drifts on divertor detachment in DIII-D with UEDGE

A.E. Jaervinen, S.L. Allen, M. Groth¹, A.G. McLean, T.D. Rognlien, C.M. Samuelli,
A. Briesemeister², M. Fenstermacher, D.N. Hill³, A.W. Leonard³, and G.D. Porter
Lawrence Livermore National Laboratory, Livermore, California 94550, USA

¹*Aalto University, P.O.Box 11000, FI-00076 AALTO, Finland*

²*Oak Ridge National Laboratory, Oak Ridge, Tennessee, USA*

³*General Atomics, P.O.Box 85608, San Diego, California 92186-5608, USA*

Partially detached divertor conditions are presently foreseen mandatory in ITER to reduce the heat fluxes on the divertor plasma facing materials below 10 MW/m², while operating at high fusion performance [1]. Cross-field drifts have been observed to strongly impact plasma conditions and the degree of detachment at each divertor plate for given main plasma conditions [2, 3, and reference therein]. To investigate the impact of drifts on the divertor conditions, dedicated sets of low and high confinement (L- and H-mode) plasmas with the $\mathbf{B} \times \mathbf{V}_B$ -drift direction towards (FWD. B_T) and away (REV. B_T) from the active X-point were conducted in the DIII-D tokamak [4, 5]. H-mode plasmas were carried out in a low triangularity configuration at toroidal field strength of 1.8 T and plasma current of 0.9 MA (DIII-D shot numbers 160997 – 161008, 161136 – 161151), while the L-mode plasmas were studied in a low triangularity configuration at toroidal field strength of 2.0 T and plasma current of 1.3 MA (DIII-D shot numbers 160299 – 160302, 160323 – 160327). The total heating power in the H-mode discharges is about 3.8 MW, and in the L-mode discharges 1 MW of Ohmic power with 100 ms NBI blips for C⁶⁺ temperature and density measurements. The divertor strike points (SP) were swept to obtain 2D Divertor Thomson Scattering (DTS) profiles [6]. Extreme SP sweeps were conducted in the H-mode plasmas to cover both low and high field side (LFS/HFS) divertor legs with the DTS system [4]. These plasmas were simulated with the multi-fluid code UEDGE [7]. UEDGE encompasses a Braginskii fluid plasma model with a fluid neutrals model. Magnetic and electric cross-field drifts are included and the electrostatic potential equation includes parallel electron currents with related plate boundary conditions on sheath potential. The code boundary conditions used in this study are described in [8].

In H-mode conditions in DIII-D, the low field side (LFS) divertor plate detaches at 20% lower LFS mid-plane separatrix density, $n_{e,SEP,LFS-MP}$, in REV. B_T than in FWD. B_T (Fig. 1a). In contrast, in L-mode conditions, the LFS divertor plate reaches electron temperatures less than

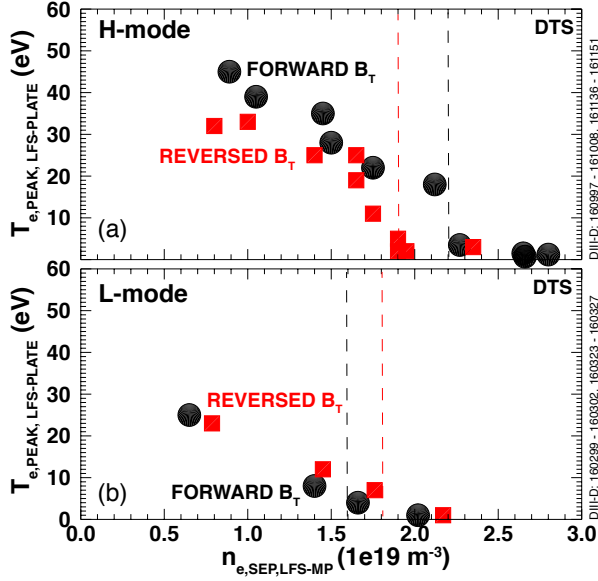


Figure 1. DTS measured LFS plate peak electron temperature as a function of LFS mid-plane separatrix electron density: a) H-mode conditions, b) L-mode conditions. The red squares stand for REV. B_T plasma and the black circles for FWD. B_T plasmas.

hand, in L-mode the poloidal particle fluxes in the divertor are dominated by recycling drive, whereas in H-mode the poloidal $\mathbf{E} \times \mathbf{B}$ drift dominates over the recycling drive [8].

Experimental measurements with the DTS system, as well as UEDGE simulations, indicate that in the L-mode conditions the radial $\mathbf{E} \times \mathbf{B}$ drift in the divertor shifts particles from the far SOL towards the separatrix in the LFS divertor leg in FWD. B_T (Figs. 2a,b,e,f). As a result, electron densities and radiation levels are increased and electron temperatures reduced close to the LFS strike point for a given upstream density. This facilitates onset of LFS detachment at lower $n_{e,SEP,LFS-MP}$ than in REV. B_T , as is observed experimentally. In REV. B_T , the radial $\mathbf{E} \times \mathbf{B}$ drift in the LFS divertor leg is reversed, shifting particles from the strike point region towards the far SOL (Figs. 2c,d). As a result, the strike point densities and radiation levels are reduced for a given upstream density, increasing the detachment threshold $n_{e,SEP,LFS-MP}$, as is observed experimentally.

In H-mode conditions, experimental measurements with the DTS in both divertor legs and UEDGE simulations indicate that strong poloidal $\mathbf{E} \times \mathbf{B}$ drift in the private flux region shifts particles from the LFS divertor to HFS divertor in the FWD. B_T (Figs. 3a,b,e,f). As a result, the LFS divertor densities and radiation levels are reduced for a given upstream density, therefore, increasing the detachment threshold $n_{e,SEP,LFS-MP}$ in FWD. B_T , as is observed experimentally. Reversing the toroidal field reverses the direction of these $\mathbf{E} \times \mathbf{B}$ drifts. As a result, in REV. B_T the LFS divertor densities and radiation levels are increased for a given

5 eV at 10% higher $n_{e,SEP,LFS-MP}$ in REV. B_T than in FWD. B_T (Fig. 1b). These trends are also qualitatively observed in UEDGE simulations including magnetic and electric drifts and SOL currents. The UEDGE simulations indicate that the relatively stronger poloidal $\mathbf{E} \times \mathbf{B}$ drifts in the H-mode conditions lead to the observed difference of the impact of field reversal on the LFS detachment threshold in L- and H-mode condition. In both L- and H-mode conditions the radial $\mathbf{E} \times \mathbf{B}$ drifts dominate over the radial diffusive fluxes in the simulations [8]. On the other

upstream density, therefore, reducing the detachment threshold density, $n_{e,SEP,LFS-MP}$, as is observed experimentally.

In H-mode conditions, UEDGE predicts radial electric fields of the order of 7kV/m in the private flux region next to the separatrix. These values are consistent with previous reciprocating probe measurements in DIII-D in H-mode conditions, published by Boedo *et al.* [10]. With the toroidal field strength of 1.8 T, this results into poloidal $\mathbf{E} \times \mathbf{B}$ drift velocity of the order of 3.5 – 4.0 km/s from the LFS to HFS in FWD. B_T configuration, reversing with the toroidal field reversal. The recycling process in the divertor leads to near sonic parallel- \mathbf{B} flows towards the nearest divertor plate. At divertor temperatures around 20 eV, the sonic flows of deuterium are of the order 50 km/s. With a B_{POL}/B_{TOT} ratio of a few per cent, this results into poloidal recycling driven flow component of the order of 0.5 – 2.5 km/s. Therefore, as is observed in the simulations, one would expect radial electric fields of the order of 7kV/m to lead to poloidal $\mathbf{E} \times \mathbf{B}$ drifts dominating over recycling driven flows. These strong poloidal $\mathbf{E} \times \mathbf{B}$ drifts lead to particle transport between the divertor legs, increasing detachment threshold density in FWD. B_T and reducing it in REV. B_T , as is observed experimentally. In the simulated L-mode conditions, the radial electric fields in the private flux region are less than 1kV/m. As a result, the poloidal $\mathbf{E} \times \mathbf{B}$ drift flux remains lower than the poloidal component of the recycling driven particle flux in the divertor legs, and strong in-out asymmetric transport in the private flux region does not occur. In these conditions, the radial $\mathbf{E} \times \mathbf{B}$ drifts can reduce the LFS divertor detachment threshold density in FWD. B_T , by transporting particles radially towards the strike point.

This work was supported in part under the auspices of the US Department of Energy (DOE) by LLNL under DE-AC52-07NA27344 and by the US DOE under DE-FC02-04ER54698, DE-FG02-07ER54917, DE-AC05-00OR22725, and DE-AC04-94AL85000. DIII-D data shown in this paper can be obtained in digital format by following the links at https://fusion.gat.com/global/D3D_DMP.

- [1] Progress in the ITER physics basis editors, Nucl. Fusion **47** (2007)
- [2] A.V. Chankin, *et al.* *J. Nucl. Mater.* **241 – 243** (1997) 199
- [3] A.V. Chankin, *et al.* *Plasma Phys. Control. Fusion* **57** (2015) 9
- [4] A.G. McLean, *et al.* *submitted to Phys. Plasmas*
- [5] M. Groth, *et al.* *Proc. of the 57th APS-DPP conf. 16-20 Nov 2015, Savannah, USA*
- [6] T.N. Carlstrom, *et al.* *Rev. Sci. Instrum.* **68** (1997) 1195.
- [7] T.D. Rognlien, *et al.* *Phys. Plasmas* **6** (1999) 1851
- [8] A.E. Jaervinen, *et al.* *submitted to Nucl. Mat. Ene.*
- [9] A.G. McLean, *et al.* *J. Nucl. Mater.* **463** (2015) 533 – 536
- [10] J.A. Boedo, *et al.* *Phys. Plasmas* **7** (2000) 1075

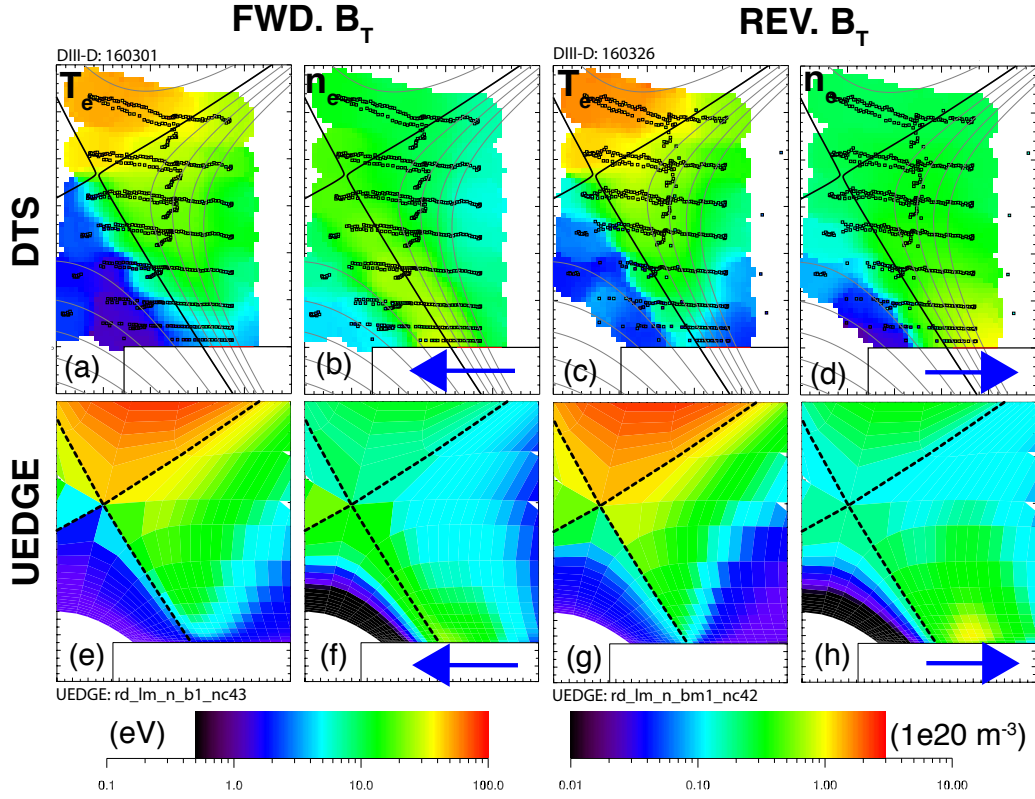


Figure 2. L-mode 2D profiles of electron temperature, T_e , and density, n_e , in the LFS divertor leg as measured by the DIII-D DTS system in FWD. B_T (a, b) (160301) and REV. B_T (c, d) (160326) configurations at $n_{e,SEP,LFS-MP}$ of about $1.65 - 1.75e19 \text{ m}^{-3}$. UEDGE predictions of 2D T_e and n_e distributions in the LFS divertor leg in FWD. B_T and REV. B_T configurations are $n_{e,SEP,LFS-MP}$ of $1.8e19 \text{ m}^{-3}$. The blue arrows represent the direction of the radial $\mathbf{E} \times \mathbf{B}$ drift in the LFS divertor leg.

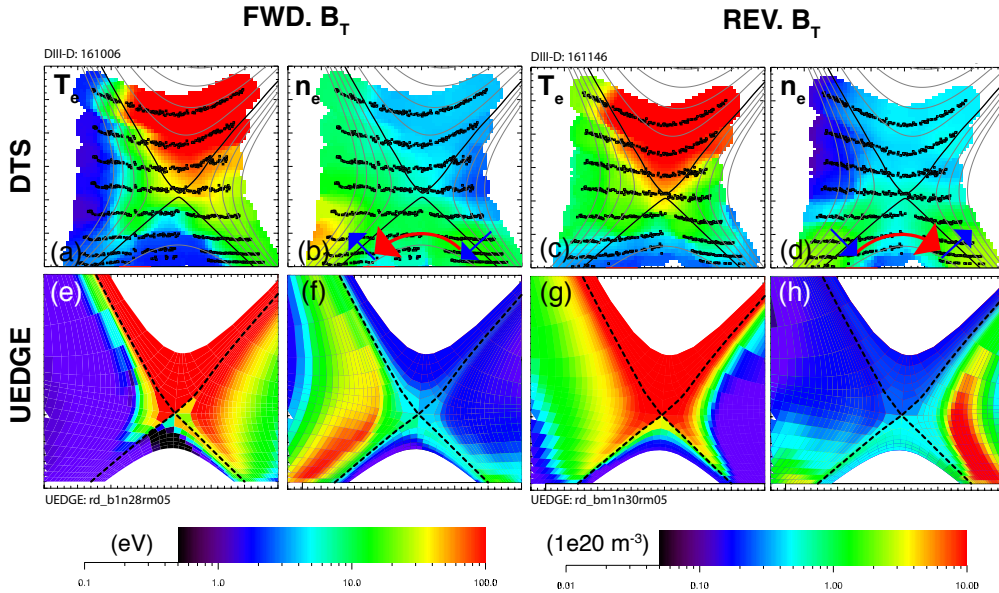


Figure 3: H-mode 2D profiles of electron temperature, T_e , and density, n_e , in the HFS and LFS divertor legs as measured by the DIII-D DTS system in FWD. B_T (a, b) (161006) and REV. B_T (c, d) (161146) configurations at $n_{e,SEP,LFS-MP}$ of about $2.1e19 \text{ m}^{-3}$ and $1.9e19 \text{ m}^{-3}$, respectively. UEDGE predictions of 2D T_e and n_e distributions in the HFS and LFS divertor legs in FWD. B_T and REV. B_T configurations are $n_{e,SEP,LFS-MP}$ of $2.7e19 \text{ m}^{-3}$. The blue arrows represent the direction of the radial $\mathbf{E} \times \mathbf{B}$ drift in the HFS and LFS divertor legs, and the red arrow represents the direction of the poloidal $\mathbf{E} \times \mathbf{B}$ drift in the private flux region.